

Thermal stability and the origin of perpendicular anisotropy in amorphous Tb-Fe-Co films

Y. J. Wang and Q. W. Leng

Institute of Physics, Chinese Academy of Sciences, Beijing 100080, People's Republic of China

(Received 7 November 1988; revised manuscript received 5 June 1989)

Both the thermal stability of the material parameters and the effect of annealing on magnetic anisotropy have been investigated for amorphous Tb₂₇Fe₅₃Co₂₀ films. On the basis of the coexistence of the pseudodipolar interaction and the stress coupled with magnetostriction, a numerical computation is performed on fitting the change of the perpendicular anisotropy K_u with temperature and K_u variations affected by annealing at the various temperatures, respectively. We show that the anisotropy originates from both the internal stress and the pseudodipolar interaction with the anisotropic part of the Ruderman-Kittel-Kasuya-Yosida exchange interaction, in which a contribution from Tb-Fe atom pairs is dominant. The change of the material parameters occurs after relatively short annealing. We attribute it to the thermal relaxation of internal stress at lower temperatures.

INTRODUCTION

Amorphous rare-earth-transition-metal (RE-TM) films are considered as a promising medium for magneto-optical recording.^{1,2} Recently, their magnetic properties have been studied actively, but problems still arise concerning the long-term stability and understanding the mechanism of the perpendicular anisotropy.

With respect to the origin of the perpendicular anisotropy, authors have published many papers on models explaining it since the amorphous Gd-Co films were successfully prepared in 1973.³ Most workers find that the perpendicular anisotropy is due to one of the following: (a) pair ordering,⁴ (b) stress-induced anisotropy,⁵ (c) bond-orientation anisotropy,⁶ (d) exchange anisotropy,⁷ or (e) the single-ion model.⁸

The internal stress may play a role, partially to determine the perpendicular anisotropy due to its coupling with magnetostriction. However, the most likely mechanism of the perpendicular anisotropy in RE-TM films is considered to be a local short-range order (LSRO). In recent years, the primarily differential anomalous x-ray scattering using synchrotron radiation has shown that the atomic-bond orientational anisotropy (ABOA) is present in Tb-Fe films,⁶ and it may be responsible for the formation of the perpendicular anisotropy. As far as the atomic bond is concerned, there are two types of interactions between the nearest atoms, Coulomb electrostatic interaction and magnetostatic interaction. For the former, a point-charge model (considering the Coulomb interaction between $4f$ electrons) was proposed⁸ to explain the perpendicular anisotropy energy in the amorphous (Gd_{0.75}R_{0.25})₁₉Co₈₁ films, here R represents rare-earth elements. However, this model cannot successfully explain the anisotropy energy about 5×10^5 erg/cm³ in Gd-Co. If the magnetostatic interaction between atoms is taken into account, then it is called the pair-ordering model, which is usually utilized to describe the perpendicular anisotropy for the amorphous RE-TM films.^{9,10} As for the exchange model, the experimental evidence is

only the behavior of rotational hysteresis W_r (the energy loss per cycle per unit volume of magnetic material, determined from a torque curve) in Gd-Co; namely, a nonvanishing value of W_r is obtained for fields greater than H_k . However, such a nonvanishing W_r was observed in the sputtered Co-Ni film¹¹ and in the magneto-optical Mn-Bi-Al-Si film¹² as well. The origin of anisotropy for these films is quite different from Gd-Co. Co-Ni possesses an induced in-plane anisotropy, but Mn-Bi-Al-Si has a crystalline anisotropy. Although the exchange anisotropy could be responsible to K_u in Gd-Co; however, there are many other reasons, such as stress, impurities, defects, dislocations, orientation imperfection of crystal structure, and dispersion of uniaxial anisotropy to influence the rotational hysteresis W_r .

The structure of amorphous RE-TM films is unstable, thus, the material parameters K_u , H_c , and θ_k may be degraded as the medium is repeatedly heated by a laser. Since this point is very important for applications, many authors have reported some results.^{13,14} But the relation between the structural relaxation and the material parameters was still not well understood.

In this paper, we study the sputtered Tb-Fe-Co film and report the thermal stability and the effect of annealing on magnetic properties for such film. In the framework of the coexistence of pair ordering and the stress, the source of the perpendicular anisotropy will be discussed. As for the pair ordering, Cargill and Mizoguchi⁴ gave the K_u expression for amorphous RE-TM films, considering it as an assembly of classical dipolar interactions. On the basis of their calculation, we assume that the contribution to K_u from Ruderman-Kittel-Kasuya-Yosida (RKKY) interactions between RE-TM atoms should be considered. In this model the pair ordering between RE(Tb)-TM(Fe,Co) atoms in Tb-Fe-Co film consists of two parts: (a) the classical atom-pair ordering taking account of the direct magnetostatic interaction between the six atom pairs, and (b) the pseudodipolar interaction considering RKKY indirectly exchange interactions between only RE-RE and RE-TM atoms.

EXPERIMENTS

Amorphous Tb-Fe-Co films with a thickness of about 200 nm were prepared by dc magnetron sputtering onto glass substrates cooled by liquid nitrogen. The sputtering rate was approximately 10 nm/min. The target was composed of a pure iron disc 65 mm in diameter and the small pure terbium and cobalt pieces were put on the disc. All Tb-Fe-Co samples were coated with a protective layer of aluminum around 500 nm.

Composition of the films was determined by electron microprobe analysis. Saturation magnetization M_s , coercivity H_c , and perpendicular anisotropy constant K_u were measured by a vibrating sample (and a sensitive torque) magnetometer with a maximum applied field up to 10 kOe, respectively. The Kerr rotation angle θ_k and Kerr hysteresis loops of the films were obtained by a polar Kerr effect meter, with maximum field greater than 8 kOe. Film thickness was measured with a surface profile system.

Thermal treatment of the samples was performed in a vacuum chamber with about 1×10^{-5} torr, and after annealing all the measurements for K_u , M_s , θ_k , and H_c were made at room temperature. Auger-electron spectroscopy (AES), x-ray photoemission spectroscopy (XPS), x-ray, and reflective-electron diffraction were used to check on the oxidation condition and the structural change of films before and after annealing.

RESULTS

It is well known that thermal magnetic writing is utilized for recording data onto magneto-optical disc. Therefore, it is very important to study thermal stability of the recording media.

Figures 1–3 show the results of the irreversible changes of K_u , θ_k , and H_c of the Tb₂₇Fe₅₃Co₂₀ film with the annealing time at the temperatures 100, 120, 150, 170, and 200°C, respectively.

The experiments indicate that K_u , H_c , and θ_k remain

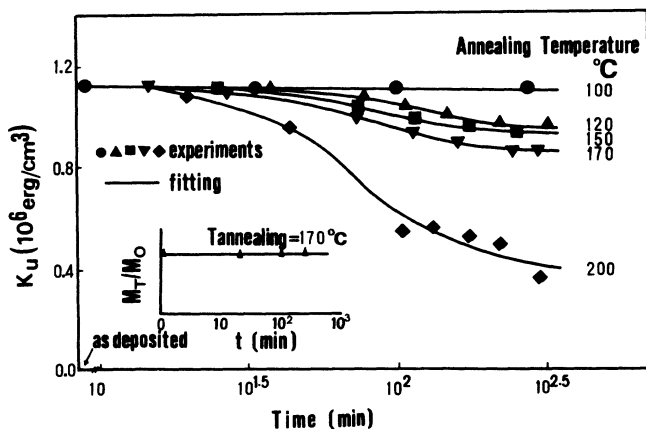


FIG. 1. The perpendicular anisotropy K_u vs annealing time t as a function of the annealing temperature T . The reduced magnetization M_T/M_0 vs t at the annealing $T = 170^\circ\text{C}$ is indicated in the inset.

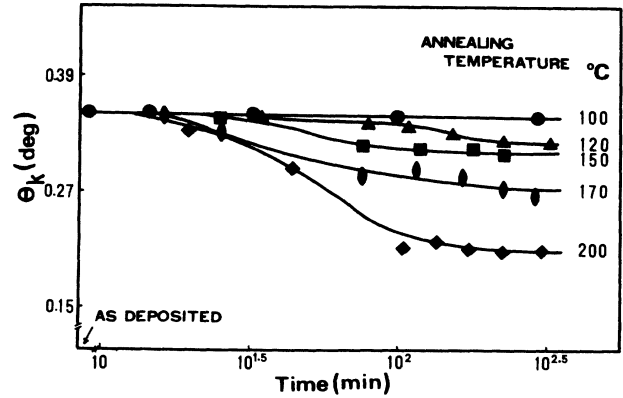


FIG. 2. The Kerr rotation angle θ_k vs the annealing time t as a function of the annealing temperature T .

constant up to about 20 min annealing at the various temperature; thereafter, K_u , H_c , and θ_k degrade for all the annealing temperatures except 100°C . The reduced magnetization M_T/M_0 , where M_0 and M_T are the saturation magnetization measured at room temperature before and after annealing, is shown in the inset of Fig. 1, and it is unchanged. Figure 4 shows the dependence of the perpendicular anisotropy K_u on temperature.

In the sample, the oxygen concentration determined by the AES profile measurements was unchanged before and after annealing; here the AES profile for after annealing only is given in Fig. 5. The XPS results illustrated in Figs. 6 show that there were no peak shifts of the Tb 4*f*, Fe 2*p*, Co 2*p* in the spectra after the samples were annealed at 170°C for 286 min. Therefore, we can deduce that the original chemical structure and the oxidation state of the elements in the sample were not affected by annealing. In addition, the results of x-ray diffraction obtained before and after thermal treatments at 100 and 170°C , respectively, appears to give no visible differences in their structure as well, as shown in Fig. 7.

In order to confirm the effect of stress on K_u as found

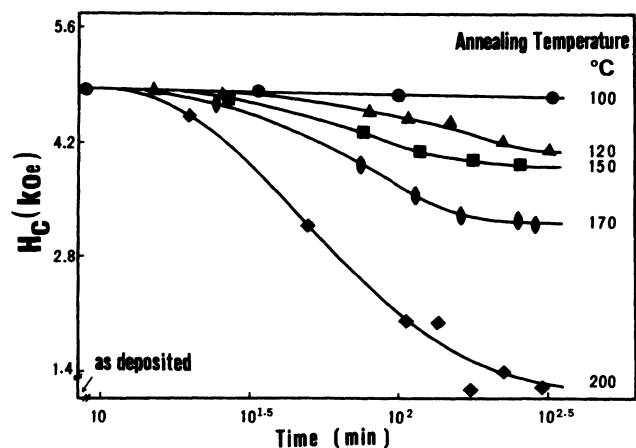


FIG. 3. The coercivity H_c vs annealing time t as a function of the annealing temperature T .

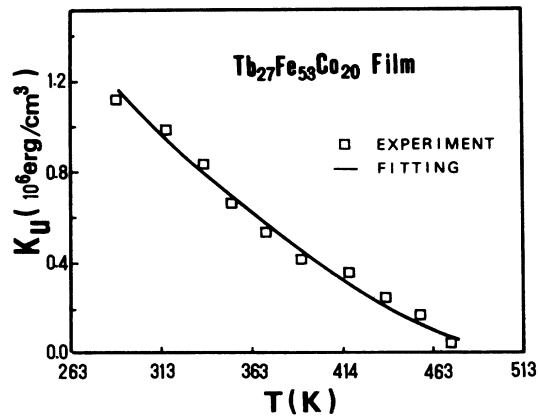


FIG. 4. The perpendicular anisotropy K_u vs temperature T .

in the study of Hashimoto *et al.* on Tb-Fe-Co film, we compared the changes of H_c and θ_k for both Tb-Fe-Co and Gd-Tb-Fe films before and after they were elastically bent. The results, given in Table I, show that θ_k did not vary for both films, and that H_c in Tb-Fe-Co for the bend state was 20% less than that for the unconstrained one, but almost unchanged for Gd-Tb-Fe within the experimental error. Here, the external applied stress expressed by the various radii of curvature for the film bending corresponds to approximately 10^{-8} dyn/cm. On the other hand, the magnetostriction coefficient λ in $\text{Tb}_{27}\text{Fe}_{53}\text{Co}_{20}$ estimated from literature¹⁵ is as high as 3.0×10^{-4} . Therefore, the stress contribution to K_u should be taken into account.¹⁶

DISCUSSION

It is known that the minimum stable domain size d_{\min} can be expressed by the formula:¹⁷

$$d_{\min} = 4(AK_u)^{1/2} / M(H_c - H), \quad (1)$$

where H is an applied magnetic field and A is an ex-

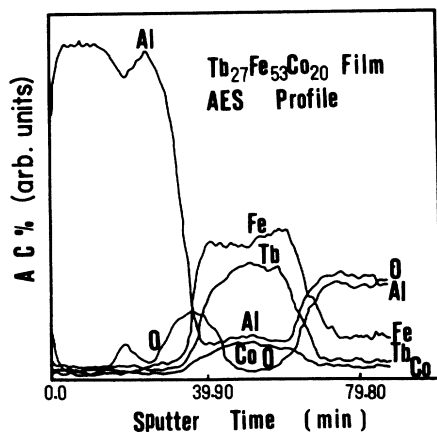


FIG. 5. The AES profile made after annealing at 170°C for 286 min.

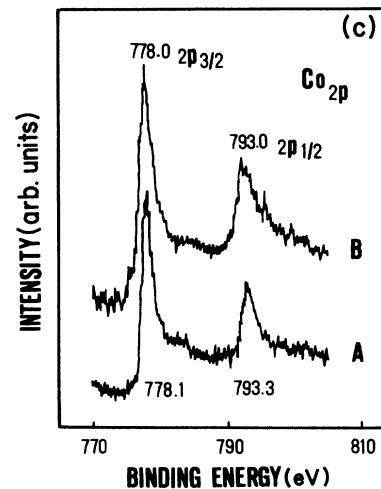
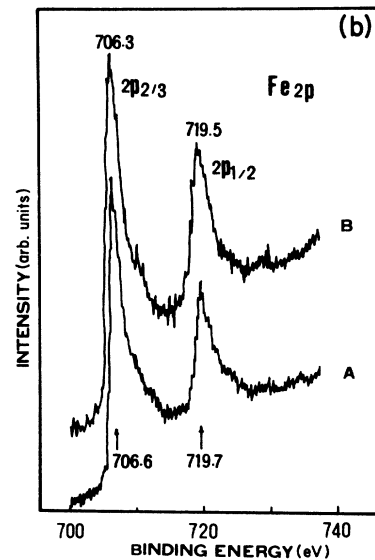
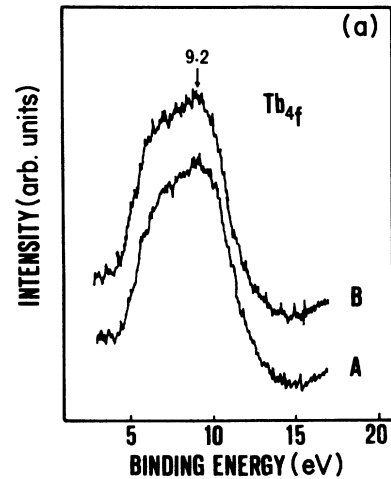


FIG. 6. XPS (a) for Tb 4f, (b) for Fe 2p, (c) for Co 2p. Here, the *A* indicates the as-deposited state, and *B* the state after annealing at 170°C for 286 min.

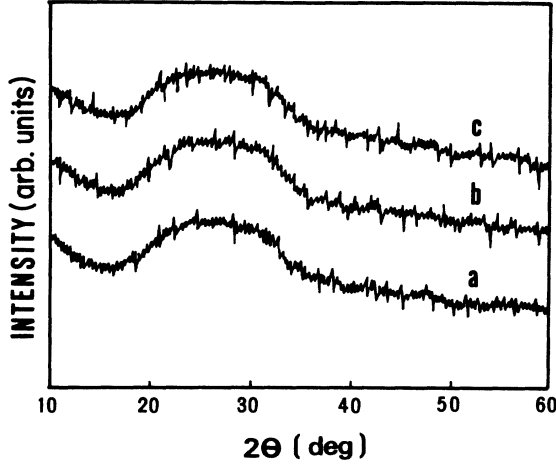


FIG. 7. The x-ray diffraction patterns. (a) As deposited, (b) after annealing at 100°C for 270 min, and (c) after annealing at 170°C for 286 min.

change constant. In addition, the ratio of output signal to noise (SNR) depends on $\theta_k R^{1/2}$, where R is the reflectivity of the film. Therefore, the thermal stability of the material parameters is required for gaining stable d_{\min} and SNR in repeated thermal writing or erasing.

From the above criteria and the results (K_u , H_c , and θ_k are constant for annealing at the various T for times less than 20 min), it should be possible to write-erase the data on the Tb-Fe-Co over one million times if each period of laser write-erase takes approximate 100 ns. However, it can be seen from the annealing results that the long-term stability of the material parameters for Tb₂₇Fe₅₃Co₂₀ still is a problem. According to calculation with mean-field theory, A is 3.7×10^{-7} erg/cm for Tb₂₇Fe₅₃Co₂₀ at room temperature. If the experimental values K_u , H_c and the theoretical value A are substituted into Eq. (1), d_{\min} should be less than 1 μm . Thus the Tb-Fe-Co film investigated here seems to be suitable for high-density recording in the sense of both the thermal stability and the appropriate size of the writing domains.

With respect to the source of the perpendicular anisotropy in the Tb₂₇Fe₅₃Co₂₀ films we use the atom-pair model associated internal stress to explain it, as discussed in the Introduction. We have the K_u expression as follows,

$$K_u = K_u^\alpha + K_u^\sigma, \quad (2)$$

TABLE I. The dependence of H_c and θ_k on stress in Tb-Fe-Co and Gd-Tb-Fe films.

Stress (Radius of the curvature mm)	Tb-Fe-Co		Gd-Tb-Fe	
	H_c (kOe)	θ_k (deg)	H_c (kOe)	θ_k (deg)
∞	2.84	0.20	2.13	0.19
150	2.29	0.20	2.18	0.19
80	2.20	0.20	2.14	0.19

where K_u^α is the atom-pair ordering part and $K_u^\sigma = -3\lambda\sigma/2$ is the stress part; λ is the magnetostriction coefficient and σ is the stress. As mentioned above, the first term on the right in Eq. (2) is composed of the classical anisotropic dipolar interaction and the anisotropic part of the RKKY interaction. We express the perpendicular anisotropy K_u^α for a ternary Tb-Fe-Co system as follows:

$$K_u^\alpha = - \sum_{i < j} \frac{X_i X_j p z}{5\mu_B g_i g_j N} \left[\left(\frac{M_i}{X_i} \right)^2 D(r_{ij}) + 2 \frac{M_i M_j}{X_i X_j} D(r_{ij}) + \left(\frac{M_j}{X_j} \right)^2 D(r_{ij}) \right]. \quad (3)$$

Here the interaction parameter $D(r_{ij})$ is

$$\begin{aligned} D(r_{ij}) &= -3g_i g_j [f(r_{ij})\mu_B^2 + J(r_{ij})] \\ &= -3g_i g_j \{ \mu_B^2 r_{ij}^{-3} - B_{ij} r_{ij}^{-4} [2k_F r_{ij} \cos(2k_F r_{ij}) \\ &\quad - \sin(2k_F r_{ij})] \}, \quad (4) \end{aligned}$$

where the first term $f(r_{ij})\mu_B^2$ in the square bracket of Eq. (4) arises from the classical dipolar interaction and the second term $J(r_{ij})$ from the RKKY interaction. $i, j=1, 2, \text{ and } 3$ and indicate Tb, Fe, and Co, respectively; r_{ij} is the distance between the nearest-neighbor atoms, N is the density of atoms; $X_i = N_i/N$, g_i , and M_i are the concentration, g -factor, and subnetwork magnetization of i -type atoms, respectively; N_i is the density of i -type atoms; k_F is the Fermi vector; p is a probability of the anisotropic orientation of the atomic pairs⁴ and $Z = Z_{ij}/X_j$, $i, j=1, 2, \text{ and } 3$. Here, Z_{ij} is the average number of j -type atoms in the nearest neighbor coordination shell of i -type atoms.¹⁸ B_{ij} is a constant determined by the interactions between a local $4f$ electron and a conduct electron under the free electron approximation. Following Yosida¹⁹ the exchange interaction $J(R)$ has the form

$$J(R) = (9\pi/4) [j_{f-s}^2(0)/E_F] F(2k_F R), \quad (5)$$

where R is the distance between two nearest-neighbor $4f$ electrons; $j_{f-s}(0)$ the exchange interaction between a $4f$ and a conductive electron and

$$F(2k_F R) = [\sin(2k_F R) - 2k_F R \cos(2k_F R)] / (2k_F R)^4 \quad (6)$$

Comparing Eqs. (4) and (5), the parameters B are equal to

$$B = (9\pi/64) \frac{j_{f-s}^2(0)}{E_F} k_F^{-4} \quad (7)$$

using $j_{f-s}(0) \approx 0.1$ eV for a free Mn ion¹⁹ and $k \approx 10$ cm^{-1} , then $B = 4 \times 10^{-47}$ for the case where the indirect exchange interaction is deduced from Eq. (7). The fitting parameter B (Tb-Tb) in the next numerical calculation of K_u^α should coincide with this value.

Generally, thermal treatment can release stress. In light of research on metglasses done by Luborsky and Walter,²⁰ the relaxation of stress follows by the relation

TABLE II. The parameters for the numerical computation.

Chemical concentration	$x(\text{Tb})=0.27$ $x(\text{Fe})=0.53$ $x(\text{Co})=0.20$
Atomic distance (Refs. 23–25)	$r(\text{Tb-Tb})=3.56 \text{ \AA}$ $r(\text{Tb-Fe})=3.03 \text{ \AA}$ $r(\text{Tb-Co})=3.04 \text{ \AA}$ $r(\text{Fe-Fe})=2.50 \text{ \AA}$ $r(\text{Fe-Co})=2.50 \text{ \AA}$ $r(\text{Co-Co})=2.50 \text{ \AA}$
Anisotropic parameter (Ref. 18)	$p=0.004$
Fermi vector (Ref. 18)	$k_F=1.30 \times 10^8 \text{ cm}^{-1}$
Average atom number in the nearest- neighbor coordinate	$z=12$
Lande factor (Refs. 25 and 26)	$g(\text{Tb})=2.00$ $g(\text{Fe})=1.93$ $g(\text{Co})=2.22$
Fitting parameters	
RKKY interaction	$B(\text{Tb-Tb})=4.93 \times 10^{-48} \text{ erg}$ $B(\text{Tb-Fe})=1.52 \times 10^{-45} \text{ erg}$ $B(\text{Tb-Co})=-5.84 \times 10^{-45} \text{ erg}$
Stress parameters	$T_0=138.3 \text{ K}$ $E_0=3.78 \times 10^5 \text{ erg/cm}^3$

$$\sigma = \sigma_0 \exp(-t/\tau), \quad (8)$$

where t is time and $\tau = \tau(T)$ is a relaxation time that depends on temperature. Since the magnetostriction coefficient depends mainly on the structure we assume for simplicity that it does not change during the annealing process, and the stress part of the contribution to K_u is

$$K_u^\sigma = E_0 \exp(-t/\tau) \exp(-T/T_0), \quad (9)$$

where

$$E_0 = -3\lambda\sigma_0/2. \quad (10)$$

In terms of the above expressions of K_u , a numerical calculation was carried out. For this calculation, we first fitted the dependence of the temperature on K_u (see Fig. 4), taking E_0 , T_0 , and B as fitting parameters. The other constants used in the fitting procedure are summarized in Table II. It is noticed that in Eq. (3) the subnetwork magnetization $M_i(T)$ ($i=1, 2$, and 3) to be used in the fitting K_u versus T was given by calculation of a mean-

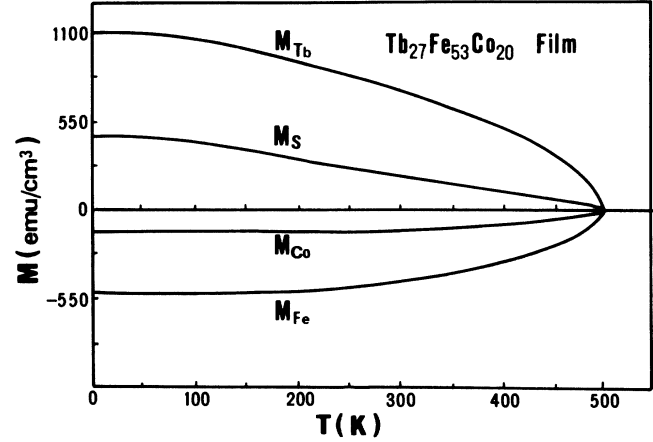


FIG. 8. The temperature dependence of the total saturation magnetization and the respective sublattice magnetization for $\text{Tb}_{27}\text{Fe}_{53}\text{Co}_{20}$ film given by the calculation of the mean-field model.

field theory, and these results, namely, the temperature dependence of M_i ($i=1, 2$, and 3), is shown in Fig. 8. The solid line in Fig. 4 is the best fitting curve for K_u , and it agrees well with the experiments. The interaction parameters D (dip), D (RKKY), and D (dip+RKKY) in Eq. (4) given by the best fitting are listed in Table III. It is obvious from the fitting parameters in Table II that K_u^σ is equal to $3.78 \times 10^5 \text{ erg/cm}^3$ and the total k_u is equal to $1.14 \times 10^6 \text{ erg/cm}^3$; hence, the contribution of stress to K_u can compare to that of the atom-pair ordering. Furthermore, in the pair-ordering part, the anisotropic RKKY interaction gives the main contribution to K_u^α and the largest contribution to K_u^α comes from Tb-Fe pairs. This point agrees with our previous work.²¹ In addition, the fitting parameter $B(\text{Tb-Tb})=4.93 \times 10^{-48}$ agrees approximately with the value given by Eq. (7), and the fitting values $B(\text{Tb-Fe})$ and $B(\text{Tb-Co})$ are larger than $B(\text{Tb-Tb})$. This is reasonable if their different environments for the exchange interactions are taken into account.

Secondly, we fitted the perpendicular anisotropy K_u expressed by Eq. (2) to the experimental annealing results (see Fig. 1). We assume that during the annealing process, stress relaxes with the annealing temperature and time according to the Eq. (9), and that the atomic nearest distance r_{ij} and the parameter p are somewhat changed, which were treated the same way as in our previous

TABLE III. The interaction parameters.

Pairs type	D (dip)	D (RKKY)	D (dip+RKKY)
Tb-Tb	-2.89×10^{-17}	-3.42×10^{-16}	-3.65×10^{-16}
Tb-Fe	-3.58×10^{-17}	-2.48×10^{-14}	-1.48×10^{-14}
Tb-Co	-4.08×10^{-17}	1.19×10^{-13}	1.19×10^{-13}
Fe-Fe	-6.15×10^{-17}	0	-6.15×10^{-17}
Fe-Co	-7.08×10^{-17}	0	-7.08×10^{-17}
Co-Co	-8.14×10^{-17}	0	-8.14×10^{-17}

TABLE IV. Fitting parameters for annealing.

T (°C)	100	120	150	170	200
τ (min)	∞	220	125	110	77

work.²¹ The final results of the numerical calculation are given in Fig. 1 with solid curves that are in good agreement with the experimental results as well. The best fitting parameters of τ , p , and r_{ij} given during the computation procedure, are indicated in Table IV and in Figs. 9 and 10, respectively.

From Fig. 9, the distance between the atom pair decreases with the increase of the annealing temperature and time. This is reasonable, since amorphous alloys are usually less dense than their crystalline counterparts. In the fitting procedure $p=0.004$ was utilized.⁴ This means that only 0.4% atom pairs contribute to K_u^α . In addition, it can be seen in Fig. 10 that the fitting value of p has a little change during the annealing procedure. These results show that the preferential orientation of the atomic pairs were influenced by annealing. Therefore, the change of properties is mainly due to the thermal stress relaxation and/or via the decrease of nearest atomic distance. But, in the case of annealing at 200°C, p degrades drastically and tends to equilibrium for relatively longer annealing times. This could be the reason why the atomic pair orderings is destroyed mostly by thermal annealing at near Curie temperature of the film.²²

It is noticed that we divided the fitting mentioned above into two steps, so as to explain the procedure of the numerical calculation conveniently. In practice the fitting was done iteratively, that is, the fitting parameters obtained by the first step were checked on the second step, namely fitting the curves of K_u versus annealing at the various temperatures. Such repeated iterations were made until the best fit, as shown in Fig. 1, and Fig. 4 was obtained simultaneously.

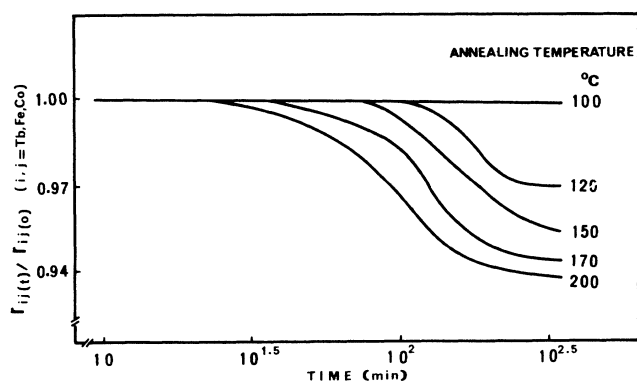


FIG. 9. The fitting parameter $r_{ij}(t)/r_{ij}(0)$ vs annealing time t as a function of the annealing temperature T .

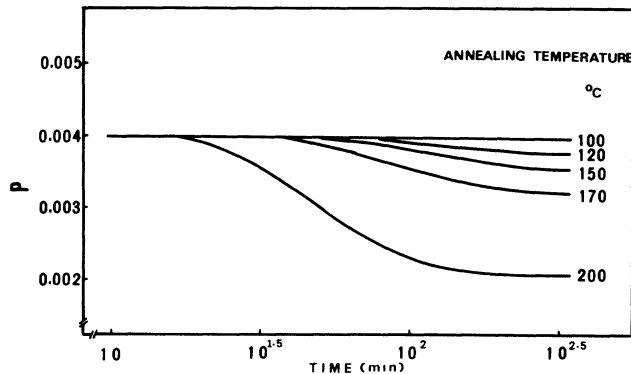


FIG. 10. The anisotropic parameter p vs annealing time t as a function of temperature T .

CONCLUSION

The amorphous $\text{Tb}_{27}\text{Fe}_{53}\text{Co}_{20}$ film prepared by magnetron sputtering possesses good thermal stability, which is required for the application of magneto-optical recording, but long term stability is still troublesome.

The perpendicular anisotropy K_u in this film originates from both the stress and the anisotropic RKKY interaction of the atom pairs. It is noticed that the Tb-Fe atom pairs in the RKKY interaction are dominant in determining K_u^α . The pseudodipolar interaction is believed to be the combined effect of spin-orbit interaction and RKKY exchange interaction. A part of the orbit will rotate with a rotation of the spin magnetic moment because of a magnetic interaction between the two, and the rotation of the orbit will, in turn, change the overlap of the wave function between the two nearest rare-earth atoms, giving rise to a change in the RKKY exchange interaction. Here, we call this type of interaction anisotropic exchange or anisotropic pseudodipolar interaction if these interactions show a preferential character in spatial distribution. Because of a very strong orbit magnetic moment, we understand why the presence of Tb atoms is very important to determine the perpendicular anisotropy.

The further degeneration of the perpendicular anisotropy K_u for long-term annealing can be attributed to stress relaxation and the changes of the anisotropic RKKY interaction of the atom pairs via the variation of the atom pairs orientation and/or the distance between atom pairs in the spatial distribution.

ACKNOWLEDGMENTS

The authors would like to thank Professor W. U. Lai for the helpful discussion, J. L. Wang and J. Y. Li for some of the magnetic measurements, and K. Xie for XPS experiments. This work was supported by the Joint Optical Disc Laboratory of the Chinese Academy of Sciences.

- ¹M. Nase, S. Yamanaka, and Y. Hoshi, *IEEE Trans. Magn.* **16**, 646 (1986).
- ²Y. Togami, K. Kobayashi, M. Kajimula, K. Sato, and T. Teranishi, *J. Appl. Phys.* **53**, 2334 (1982).
- ³P. Chaudhari, J. J. Cuomo, and R. J. Gambino, *IBM J. Res. Dev.* **11**, 66 (1973).
- ⁴G. S. Cargill and T. Mizoguchi, *J. Appl. Phys.* **50**, 3570 (1979).
- ⁵T. Katayama, M. Hirano, Y. Koizumi, K. Kawanishi, and T. Tsushima, *IEEE Trans. Magn.* **13**, 1603 (1977).
- ⁶T. Egami, C. D. Graham, Jr., W. Dmowski, P. Zhou, P. J. Flanders, E. E. Marinero, H. Notargs, and C. Robinson, *IEEE Trans. Magn.* **23**, 2269 (1987).
- ⁷W. H. Meiklejohn, F. E. Luborski, and p. G. Frischman, *IEEE Trans. Magn.* **23**, 2272 (1987).
- ⁸Y. Suzuki, S. Takayama, F. Kirino, and N. Ohta, *IEEE Trans. Magn.* **23**, 2275 (1987).
- ⁹R. B. van Dover and M. Hong, *J. Appl. Phys.* **57**, 3897 (1985).
- ¹⁰N. Sato and K. Habu, *J. Appl. Phys.* **61**, 4287 (1987).
- ¹¹X. R. Luo *et al.* (unpublished).
- ¹²Y. J. Wang *et al.* (unpublished).
- ¹³M. Hartmann, S. Klahn, and K. Witter, *IEEE Trans. Mag.* **23**, 2946 (1987).
- ¹⁴F. E. Luborsky, *J. Non-Cryst. Solids* **61/62**, 829 (1984).
- ¹⁵S. Hashimoto, Y. Ochiai, M. Kaneko, K. Watanada, and K. Aso, *IEEE Trans. Magn.* **23**, 2278 (1987).
- ¹⁶P. J. Grund and R. S. Tebble, *Adv. Phys.* **17**, 153 (1968).
- ¹⁷F. E. Luborski, *IEEE Trans. Magn.* **21**, 1618 (1985).
- ¹⁸K. Twarowski, H. K. Lachowicz, M. Gutowski, and H. Szymczak, *Phys. Stat. Sol. (a)* **63**, 103 (1981).
- ¹⁹K. Yosida, *Phys. Rev.* **106**, 893 (1957).
- ²⁰F. E. Luborski and J. L. Watter, *Mater. Sci. Eng.* **35**, 255 (1978).
- ²¹Y. J. Wang, H. Cai, Q. Tang, K. M. Yang, J. Y. Li, and J. L. Wang, *J. Magn. Magn. Mater.* **66**, 84 (1987).
- ²²R. Hasegawa, R. J. Gabino, J. J. Cuomo, and J. F. Ziegler, *J. Appl. Phys.* **45**, 4036 (1974).
- ²³G. S. Cargill, in *Magnetism and Magnetic Materials (Boston, 1973)*, Proceedings of the 19th Annual Conference on Magnetism and Magnetic Materials, AIP Conf. Proc. No. 18, edited by C. D. Graham and J. J. Rhyne (AIP, New York, 1974), p. 631.
- ²⁴A. Gangule and W. C. Taylor, *J. Appl. Phys.* **49**, 1762 (1987).
- ²⁵A. H. Eschenfelder, in *Ferromagnetic Materials*, edited by E. P. Wohlfarth (North Holland, Amsterdam, 1980), Vol. 2.
- ²⁶G. E. Roberts, W. L. Wilson, Jr., and H. C. Bourne, Jr., *IEEE Trans Magn.* **13**, 1535 (1977).